Leronlimab is associated with long-term survival in metastatic TNBC: Enhancing PD-L1 expression, ICI response, and modulates T cell exhaustion

Richard G. Pestell [1,2] , Zhiping Li [1] , Ritika Harish [1] , Danni Li [1], Xuanmao Jiao [1] , Hallgeir Rui [3] , Daniel L. Adams [4] , Max Lataillade [5] , Neil E. Buss [6] , A. Cyrus Arman [5] , Jonah B. Sacha [7,8] , Jacob P. Lalezari [5]

[1] Pennsylvania Cancer and Regenerative Medicine Research Center, Baruch S. Blumberg Institute, Wynnewood, PA; [2] The Wistar Cancer Center, Philadelphia, PA; [3] Thomas Jefferson University, Philadelphia, PA; [4] Creatv MicroTech, Inc., Monmouth Junction, NJ;

[5] CytoDyn, Inc., Vancouver, WA; [6] Nucleus Global, 4413 Büren, Switzerland; [7] Vaccine and Gene Therapy Institute, Oregon Health and Science University, Portland, OR; [8] Oregon National Primate Research Center, Oregon Health and Science University, Portland, OR

Abstract

Introduction: Metastatic triple-negative breast cancer (mTNBC) is a deadly disease in which more than 50% of PD-L1 positive patients responded to the immune check point inhibitors (ICI) pembrolizumab. Resistance mechanisms to ICI include low PD-L1 and T cell exhaustion. CCR5 abundance is increased in ~95% of mTNBC, CCR5 protein was shown on the surface of human breast cancer cells and blocking CCR5 with either small molecules (maraviroc) or a humanized monoclonal antibody (leronlimab) both prevents and reduces the size of established mTNBC in preclinical studies. The current studies were conducted to identify the molecular mechanisms by which leronlimab may govern ICI responses in mTNBC.

Methods: Analysis of patient gene expression, tissue culture and clinical trial material (tumor histology, cancer associated macrophage/circulating tumor cells (CAML/CTC) and analysis of mTNBC patient outcomes), was conducted.

Findings: (1) Analysis of four TNBC patient data sets showed a significant positive correlation between cytotoxic T lymphocyte (CTL) levels and CCR5 gene expression. In large breast cancer cohorts (N=1,094), CCR5 expression correlated strongly with T cell exhaustion signatures. The high ImmunoPhenotype Score CCR5 High was highly correlated with CCR5 in TNBC subtypes; (2) CCR5 expression on human TNBC cell lines suppressed the abundance of glycosylated PDL1; CCR5 inhibition, with either leronlimab or maraviroc, increased the abundance of PDL1 (18 kDa, 55kDa); (3) In cultured TNBC breast cancer cells, a CCR5 mediated secretome was identified. CCR5 activity induced sB7H3 (CD276) (known to promote T cell exhaustion), sTNFSF13B (BAFF), sTyro3 (linked to breast cancer ferroptosis inhibition) and Tyro3 ligand. CCR5 inhibition with either leronlimab or maraviroc reduced sB7H3, sTNFSF13B and sTyro3; (4) Leronlimab reduced T cell exhaustion markers on CD4 + and CD8 + T cells in rhesus macaque monkeys. In rhesus macaques receiving a single 50 mg/kg injection of leronlimab CCR5 receptor occupancy on lymph node resident CD8 + T cells, coincided with upregulated PD-1 expression significantly by 4 weeks post injection. In lymph node CD8 + T cells contemporaneous with peak leronlimab levels at 1 week, a decline in the percent positive cells for LAG3, TIM3 and CTLA4 was observed; (5) In a retrospective post hoc analysis including pooled data from 28 patients with mTNBC, from three clinical trials, leronlimab was well tolerated with no patients withdrawing due to leronlimab-related adverse events. After a median of over 60 months 5/28 (17.9%) of heavily pretreated mTNBC patients are currently alive (1-year survival 35.7%; 2-year survival 21.4%; 3-year survival 17.9%; 4-year survival 17.9%).

Conclusions: CCR5 may promote ICI resistance in TNBC by upregulating immune checkpoints (sB7H3, and sTyro3). Leronlimab induces PDL1 expression on CAML/CTC, which may prime tumors for successful PDL1 blockade.

1. A low prevalence of treatment-related adverse events in patients treated with leronlimab

A

Baseline characteristic	Value
Median age (Range)	48.5 (32-83)
Median prior metastatic therapies	2 (0-5[‡])
Number prior metastatic therapies	
0	2 (7%)
1	9 (32%)
2	9 (32%)
≥3	7 (25%)
Unknown	1 (4%)
ECOG	
0	18 (64%)
≥1	10 (36%)
Visceral	
None	10 (36%)
Positive	18 (64%)
Brain metastasis	7 (24%)
Prior treatment with ICI	9 (29%)
PD-L1 (CPS scores)[‡]	
<1%	8 (29%)
≥1%	18 (64%)
≥10%	5 (18%)
Unknown	2 (7%)

B

Study treatment characteristic	Value
ICI treatment with or after leronlimab	7 (25%)
Leronlimab dose	
350 mg QW SC	12 (36%)
525 mg QW SC	15 (53%)
(2 increased from 350 mg QW)	
700 mg QW SC	3 (11%)

† Unknown for one participant
‡ As identified from the patient's medical records
ICI = immune checkpoint inhibitor; QW = once weekly; SC = subcutaneously

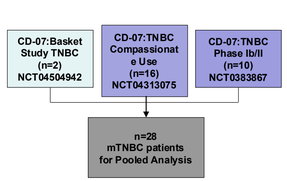

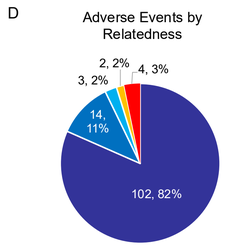

Figure 1. Leronlimab shows infrequent adverse events in clinical trial. (A) Patient characteristics from the clinical trials. (B) Dose of leronlimab used by the patents in the clinical trial. (C) Flowchart of clinical trials analyzed. (D) Pie diagram representing the total number of AEs and the total number of leronlimab-related AEs shown as either directly related or possible related to leronlimab.

2. Liquid biopsies show CCR5 pools in circulating Cancer Associated Macrophage-Like cells predict better outcome in patients treated with Leronlimab

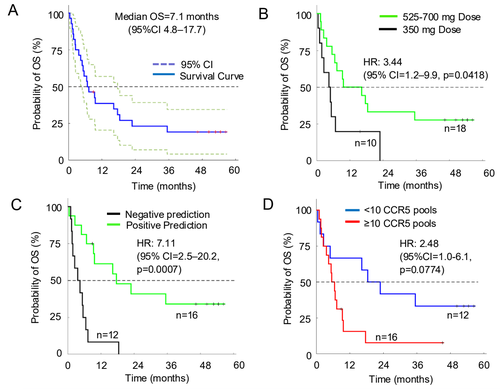

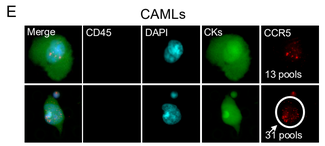

Figure 2. Predictors of patient response to leronlimab include higher therapeutic dose and lower number of CCR5 dots in Cancer Associated Macrophage Like cells. (A) Cox Proportional Hazards regression of all patients treated with leronlimab showing the OS. (B) The OS of patients based on the dose of leronlimab received by the patient (350 mg black line, 525-700 mg green line). (C) Probability of OS based on the LifeTracDx® based algorithm. Positive prediction is a decrease in either number or size of circulating cells or both, whereas negative prediction is an increase in either number or size of circulating cells. (D) The OS of patients based on the change in CTC/CAML number after administration of leronlimab (increase in CTC/CAML number-black line, decrease in CTC/CAML number-green line). Probability of OS based on change in CCR5 pools between pre (BL) and post (T1) induction of leronlimab comparing the number of dots (<10 CCR5 pools-blue line, >10 CCR5 pools-red line. Cox Proportional Hazards regression of all patients treated with leronlimab and their OS based on changes in CCR5 dots in CAMLs. (E) Representative examples of cancer associated macrophage like cells (CAMLs) CCR5 showing the number of CCR5 "pools". Blue is DAPI for nuclear identity, green is anti-cytokeratin-FITC, red is for CCR5.

3. Leronlimab induces PD-L1, corresponds to improved survival with an ICI

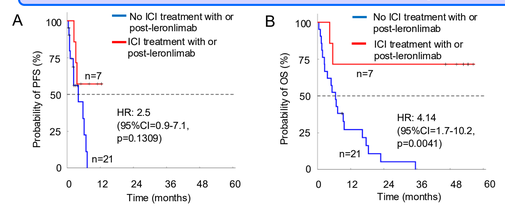

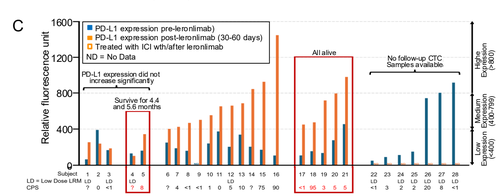

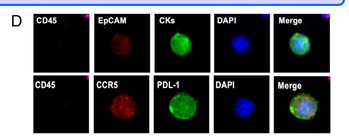

Figure 3. Leronlimab induction of PD-L1 in CAML/CTC is associated with response to immune check point inhibitors and favorable outcome. Probability of PFS (A) and OS (B) based on leronlimab treatment either with (red line) or without (blue line) an immune checkpoint inhibitor (ICI). (C). PD-L1 abundance on CAML/CTC determined by immunofluorescence either pre-leronlimab treatment (pre-LRM) or after leronlimab treatment (post-LRM). Orange square highlights patients who showed a significant induction of PD-L1 and were treated with an ICI that are currently alive (>5 years). Representative example of CTC immunofluorescence for PD-L1 and CCR5, with DAPI used to identify the nucleus and Cytokeratin as a marker of epithelial cells and CD45 as a pan leukocyte marker to define CAMLs. (D) Representative images of CTCs/CAMLs with PD-L1 expression. In the upper panel, EpCAM is shown in red and cytokeratins (CKs) in green. In the lower panel, CCR5 is shown in red and PD-L1 in green. Nuclei are counterstained with DAPI (blue) in both panels.

4. Leronlimab induces PD-1 in the lymph nodes of rhesus macaques

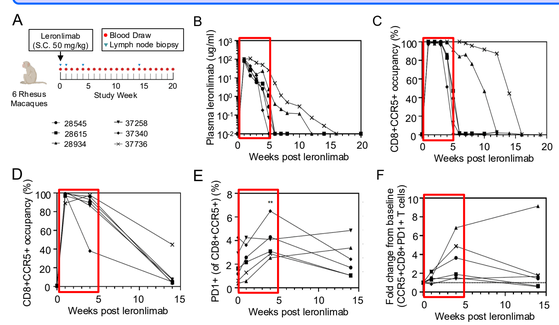

Figure 4. Leronlimab governs exhaustion marker expression in CD8+ T cells of rhesus macaques. (A) Study outline. Leronlimab-naïve rhesus macaques (n = 6) were subcutaneously administered Leronlimab to 50 mg/kg. Blood (red circles) was obtained throughout the course of the study until week 20 and lymph node biopsies (blue triangles) were collected at weeks 0, 1, 4, and 14. (B) Longitudinal plasma leronlimab in rhesus macaques. (C) Longitudinal $CD8^+CCR5^+$ receptor occupancy in blood. (D) Longitudinal $CD8^+CCR5^+$ receptor occupancy in lymph nodes. (E) Longitudinal PD1 expression in lymph node as a % of $CCR5^+CD8^+$ T cells. (F) Fold change in PD1 expression in lymph node in $CCR5^+CD8^+$ T cells vs baseline.

* Correspondence Should be address to Jacob P. Lalezari at jlalezari@cytodyn.com, CytoDyn, Vancouver, WA.

5. CCR5 correlates with markers of T cell immune exhaustion

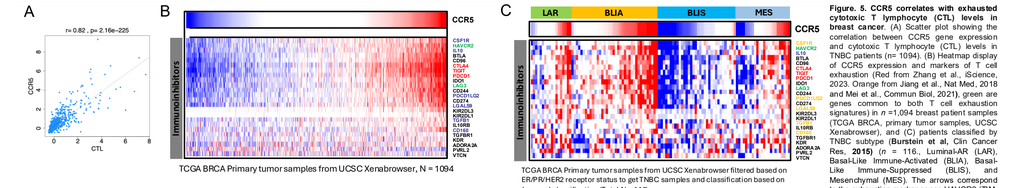

Figure. 5. CCR5 correlates with exhausted cytotoxic T lymphocyte (CTL) levels in breast cancer. (A) Scatter plot showing the correlation between CCR5 gene expression and cytotoxic T lymphocyte (CTL) levels in TNBC patients (n= 1094). (B) Heatmap display of CCR5 expression and markers of T cell exhaustion (Red from Zhang et al., iScience, 2023. Orange from Jiang et al., Nat Med., 2018 and Mei et al., Commun Biol, 2021), green are genes common to both T cell exhaustion signatures) in n =1,094 breast patient samples (TCGA BRCA, primary tumor samples, UCSC Xenabrowser), and (C) patients classified by TNBC subtype (**Burstein et al,** Clin Cancer Res, **2015**) (n = 116., Luminal-AR (LAR), BasalLike Immune-Activated (BLIA), Basal-Like Immune-Suppressed (BLIS), and Mesenchymal (MES). The arrows correspond to the exhaustion marker genes HAVCR2 (TIM-3), TIGIT, PDCD1 (PD-1), and LAG-3.

6. Indices of T cell exhaustion correlate with CCR5 in triple-negative breast cancer

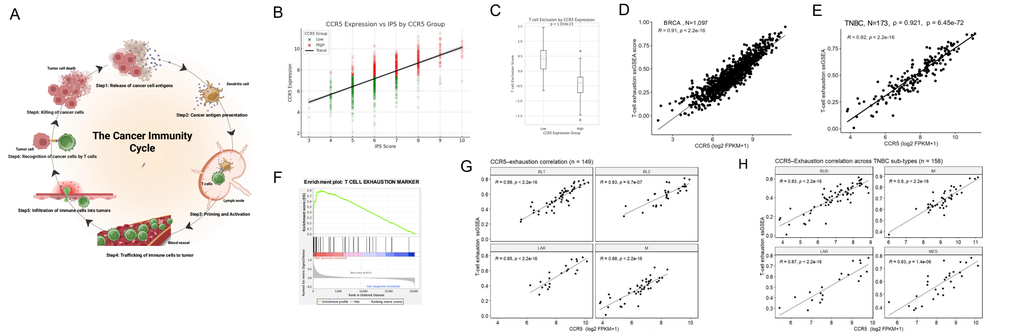

Figure 6. Indices of T cell exhaustion correlate with CCR5 in triple-negative breast cancer. (A) Schematic representation of cancer-immunity cycle. (B) Scatter plot of CCR5 expression (y-axis, $\log_2$[TPM+1]) versus ImmunoPhenotype Score (IPS) (x-axis). Points are colored by CCR5 group (green = Low, red = High; median split); the black line shows the overall ordinary least squares (OLS) trend. (Pearson correlations (two-sided): Low $r = 0.358$, $P = 5.1 \times 10^{-14}$ (n = 547); High $r = 0.585$, $P = 2.0 \times 10^{-41}$ (n = 546). The stronger positive association in the $CCR5^{High}$ stratum indicates that CCR5 tracks more closely with a high IPS score. (C) The boxplot shows the TIDE T Cell Exclusion score in $CCR5^{Low}$ (n = 94) and $CCR5^{High}$ (n = 95) TNBC samples from TCGA (TCGA-BRCA (Breast Invasive Carcinoma UCSC Xenabrowser (https://xenabrowser.net/)). The median T Cell Exclusion score was higher in $CCR5^{Low}$ group compared with $CCR5^{High}$ group, indicating reduced stromal/architectural barriers to T-cell infiltration in the $CCR5^{High}$ group (Wilcoxon rank-sum $P = 1.01 \times 10^{-89}$). Boxes depict the interquartile range with center lines at the median; outliers are shown as individual points. (D) CCR5 expression versus T-cell exhaustion, determined using the ssGSEA exhaustion score signature, in TCGA-BRCA primary tumors (UCSC Xenabrowser (https://xenabrowser.net/)). Scatterplot of CCR5 ($\log_2$ FPKM + 1) on the x-axis and the ssGSEA exhaustion score is shown on the y-axis for all primary breast cancer tumors (n = 1,097). The solid line indicates the least-squares fit. Spearman's ρ and two-sided p-value are displayed in the panel. A strong positive association indicates that tumors with higher CCR5 expression exhibit higher T-cell exhaustion signatures. (E) Scatterplot of CCR5 ($\log_2$ FPKM + 1) *vs.* ssGSEA exhaustion score defined by The Cancer Imaging Archive (TCIA) is shown for TNBC patient samples, showing a robust positive correlation (R = 0.92, P = 6.45e-72 (n = 173)) (Spearman R with a single two-sided P value). (F) GSEA enrichment plot showing significant enrichment of custom T cell exhaustion marker gene set in TCGA breast cancer TNBC (Xenabrowser) in which $CCR5^{High}$ tumors were compared to the $CCR5^{Low}$ tumors. (G) Correlation *vs.* ssGSEA exhaustion score signature for TNBC classified as Lehmann subtype, (H) or Jézéquel subtype.

7. Leronlimab governs a T cell exhaustion regulatory secretome in TNBC

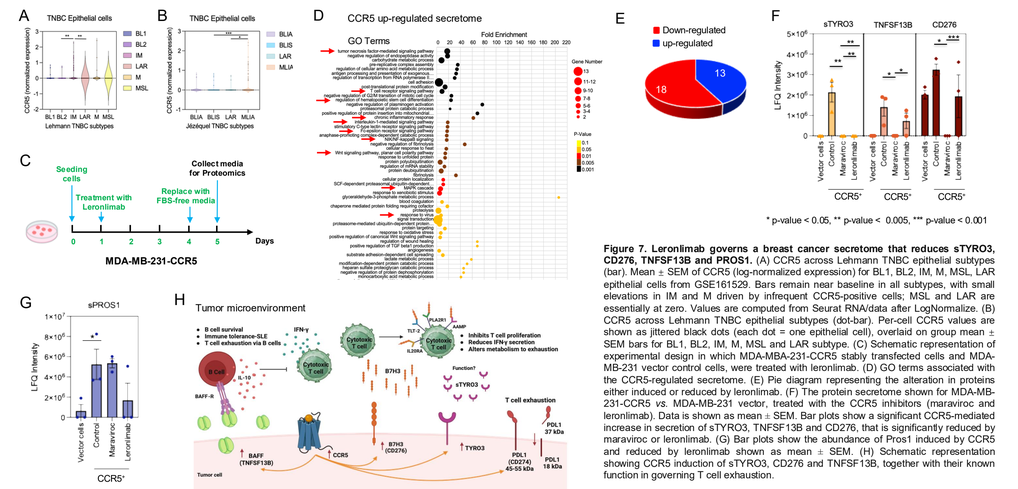

* p-value < 0.05, ** p-value < 0.005, *** p-value < 0.001

Figure 7. Leronlimab governs a breast cancer secretome that reduces sTYRO3, CD276, TNFSF13B and PROS1. (A) CCR5 across Lehmann TNBC epithelial subtypes (bar). Mean ± SEM of CCR5 (log-normalized expression) for BL1, BL2, IM, M, MSL, LAR epithelial cells from GSE161529. Bars remain near baseline in all subtypes, with small elevations in IM and M driven by infrequent CCR5-positive cells; MSL and LAR are essentially at zero. Values are computed from Seurat RNA/data after LogNormalize. (B) CCR5 across Lehmann TNBC epithelial subtypes (dot-bar). Per-cell CCR5 values are shown as jittered black dots (each dot = one epithelial cell), overlaid on group mean ± SEM bars for BL1, BL2, IM, M, MSL and LAR subtype. (C) Schematic representation of experimental design in which MDA-MBA-231-CCR5 stably transfected cells and MDA-MB-231 vector control cells, were treated with leronlimab. (D) GO terms associated with the CCR5-regulated secretome. (E) Pie diagram representing the alteration in proteins either induced or reduced by leronlimab. (F) The protein secretome shown for MDA-MB-231-CCR5 *vs.* MDA-MB-231 vector, treated with the CCR5 inhibitors (maraviroc and leronlimab). Data is shown as mean ± SEM. Bar plots show a significant CCR5-mediated increase in secretion of sTYRO3, TNFSF13B and CD276, that is significantly reduced by maraviroc or leronlimab. (G) Bar plots show the abundance of Pros1 induced by CCR5 and reduced by leronlimab shown as mean ± SEM. (H) Schematic representation showing CCR5 induction of sTYRO3, CD276 and TNFSF13B, together with their known function in governing T cell exhaustion.